DALTON
FULL PAPER

Synthesis, characterization, and spectroscopic properties of three novel pentadentate copper(II) complexes related to the metal-chelating inhibitors against DNA binding with HIV-EP1

Hiromasa Kurosaki,[a] Rakesh Kumar Sharma,[b] Sachiko Aoki,[c] Teruhiko Inoue,[d] Yoshinari Okamoto,[c] Yukio Sugiura,[d] Mitsunobu Doi,[e] Toshimasa Ishida,[e] Masami Otsuka[c] and Masafumi Goto[a]

[a] *Department of Physical Chemistry, Faculty of Pharmaceutical Sciences, Kumamoto University, 5-1 Oe-honmachi, Kumamoto, 862-0973, Japan. Fax: +81-96-371-4314; E-mail: gotomphi@gpo.kumamoto-u.ac.jp*
[b] *Department of Chemistry, University of Delhi, Delhi-7, India*
[c] *Department of Bioorganic Medicinal Chemistry, Faculty of Pharmaceutical Sciences, Kumamoto University, 5-1 Oe-honmachi, Kumamoto, 862-0973, Japan*
[d] *Institute for Chemical Research, Kyoto University, Uji, Kyoto, 611-0011, Japan*
[e] *Osaka University of Pharmaceutical Sciences, Nasahara, Osaka, 569-1094, Takatsuki, Japan*

Received 25th August 2000, Accepted 7th December 2000
First published as an Advance Article on the web 25th January 2001

Three potentially five-coordinate peptide ligands having a pyridine and two histidine moieties, were synthesized to study their copper(II) complexation. Blue copper(II) complexes with deprotonated amide groups were isolated from methanolic solutions of the corresponding ligands with equimolar $Cu(OAc)_2 \cdot H_2O$. The structures of two of them were determined by X-ray crystallography. The Cu is coordinated to five nitrogen atoms in both complexes; the coordination geometry was a distorted square pyramid in one, and intermediate between a square pyramid and trigonal bipyramid in the other. EPR spectra in frozen methanol solutions at 77 K as well as visible absorption spectra indicate that the distortion of the geometry around the copper is reduced by the introduction of an alkylamine substituent on the pyridine of the ligand and that the substituted complexes distort toward trigonal bipyramidal geometry compared to the unsubstituted one in solution.

Introduction

The design, synthesis and evaluation of new potential therapeutic agents for treatment of acquired immunodeficiency syndrome (AIDS) is a significant challenge to the medical scientific community. Treatment with multidrug therapy using recently approved potent inhibitors of HIV-1 reverse transcriptase and protease enzymes is useful only in delaying the progression of AIDS and death associated with HIV infection. However, it is now becoming clear that these cocktails are failing due to a number of reasons.[1–3] Thus, there is a clear need for the development of new antiviral agents that affect unique targets, but which do not demonstrate cross-resistance with existing drugs. In this regard we recently reported a symmetrical metal chelating system comprising pyridine and histidine methyl ester namely HPH.[4–6] These novel metal chelators are found to inhibit the binding of metalloprotein HIV-EP1 (HIV enhancer binding protein) to the NF-κB recognition sequence of DNA by ejecting metal from the metalloprotein.

So the main objective of our study is to investigate coordination modes of different pyridine and histidine methyl ester systems (HPH) for better design of anti-HIV metal chelators. We report here the synthesis, structure, and spectral properties of copper(II) complexes of the five-coordinate ligands $HPH\text{-}PepH_2$ (**1**), $BuMeN\text{-}HPH\text{-}PepH_2$ (**2**), and $Me_2N\text{-}HPH\text{-}PepH_2$ (**3**) (see Chart 1).

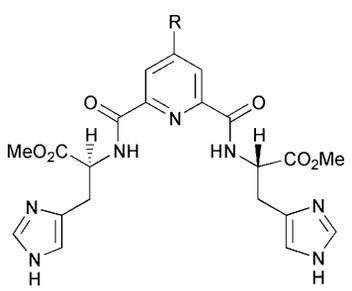

$HPH\text{-}PepH_2$; **1**: R = H
$BuMeN\text{-}HPH\text{-}PepH_2$; **2**: R = NBuMe
$Me_2N\text{-}HPH\text{-}PepH_2$; **3**: R = NMe_2

Chart 1

Experimental

General information

All the materials were of reagent grade used without further purification unless noted. Copper(II) acetate monohydrate was purchased from Wako Chemical Co. 400 MHz ^{1}H NMR spectra were recorded on a JEOL GX-400 spectrometer, and tetramethylsilane in organic solvent was used as an internal reference.

Ligand syntheses

$HPH\text{-}PepH_2$ (1). Compound **1** was prepared from 2,6-pyridinedicarboxylic acid and L-histidine methyl ester dihydrochloride using a coupling method with diphenoxyphosphoryl azide (DPPA) and triethylamine according to the published procedure.[7]

4-Chloropyridine-2,6-dicarboxylic acid (6). Phosphorus pentachloride (100 g, 0.48 mmol) was added to a suspension of chelidamic acid **4** (25 g, 0.12 mol) in chloroform (300 cm^3) at

DOI: 10.1039/b006949n

room temperature. The mixture was heated at reflux for 90 h. MeOH (200 cm^3) was slowly added to the mixture at 0 °C and the resulting solution stirred for 1 h at room temperature and neutralized with saturated aqueous $NaHCO_3$. After evaporation of MeOH *in vacuo*, insoluble material was removed by filtration and the filtrate extracted with ethyl acetate. The extract was dried over Na_2SO_4, concentrated *in vacuo* and the crystalline dimethyl 4-chloropyridine-2,6-dicarboxylate **5** deposited collected and washed with hexane. A suspension of diester **5** in 1 M NaOH was stirred at 80 °C for 2 h. The solution was cooled with ice and acidified with 1 M HCl to pH 4. The white precipitate was collected to give compound **6** in 85% yield based on **4**.

Dimethyl 4-butylmethylaminopyridine-2,6-dicarboxylate (8). A suspension of compound **6** (3 g, 14.8 mmol) in aqueous *N*-butylmethylamine (25% solution, 35 cm^3) was stirred at 150 °C for 2 h in a sealed tube. The resulting solution was concentrated *in vacuo* to give crude **7** that was used for the next step without further purification. Thionyl chloride (22.3 cm^3) was slowly added to an ice-cooled mixture of the above acid **7** in dry MeOH (100 cm^3). The solution was heated at reflux for 12 h and concentrated *in vacuo*. The residue was partitioned between saturated aqueous $NaHCO_3$ and ethyl acetate. The aqueous layer was further extracted with ethyl acetate. The extract was dried over Na_2SO_4 and concentrated *in vacuo*. The residue was purified by chromatography on silica gel with CH_2Cl_2–MeOH (2:1) to give **8** as yellow-brown oil in 70% yield based on **6**. IR (film): 3500, 2950, 1720, 1600, 1400, 1250, 1160, 1030, 780 and 730 cm^{-1}. MS(FAB): *m*/*z* 281. ^1H NMR ($CDCl_3$): δ 0.94–1.00 (2H, t, $J = 8.1$), 1.36–1.58 (2H, m), 1.60–1.66 (2H, m), 3.08 (3H, s), 3.42–3.47 (2H, t, $J = 6.8$ Hz), 3.98 (6H, s) and 7.49 (2H, s). Calc. for $C_{14}H_{20}N_2O_4 \cdot 0.5H_2O$: C, 58.12; H, 7.32; N, 9.68. Found: C, 58.17; H, 7.67; N, 9.52%.

4-Butylmethylaminopyridine-2,6-dicarboxylic acid (7). A suspension of diester **8** (1 g, 4.0 mmol) in 1 M NaOH (5 cm^3) was stirred at 80 °C for 1 h. The solution was acidified with 1 M HCl to pH 4 and concentrated *in vacuo* to give compound **7** as a white powder in quantitative yield. IR (KBr): 3450, 3320, 3260, 3080, 2955, 2930, 2870, 1615, 1580, 1520, 1410, 1360, 1280, 920, 895, 805 and 720 cm^{-1}. MS (FAB): *m*/*z* 253. ^1H NMR ($CDCl_3$): δ 0.98–1.04 (3H, t, $J = 7.26$), 1.38–1.51 (2H, m), 1.65–1.73 (2H, m), 3.32 (3H, s), 3.66–3.72 (2H, t, $J = 7.58$ Hz) and 7.51 (2H, s).

BuMeN-HPH-PepH_2 (2). Diphenoxyphosphoryl azide (0.68 cm^3, 3.17 mmol) and triethylamine (0.88 cm^3, 6.34 mmol) were successively added to a solution of compound **7** (200 mg, 0.79 mmol) and histidine methyl ester dihydrochloride (348 mg, 1.58 mmol) in DMF (10 cm^3) at 0 °C. The solution was stirred at 0 °C for 2 h then at room temperature for 3 days and concentrated *in vacuo*. The residue was partitioned between saturated aqueous $NaHCO_3$ and chloroform. The aqueous layer was further extracted with chloroform. The chloroform extract was dried over Na_2SO_4 and concentrated *in vacuo*. The residue was purified by chromatography on silica gel with CH_2Cl_2–MeOH–Et_3N (20:1:1) as eluent to give **2** as a pale yellow powder in 40% yield. IR (KBr): 3300, 2960, 1740, 1660, 1610, 1525, 1435, 1215, 1175 and 740 cm^{-1}. MS (FAB): *m*/*z* 555. ^1H NMR($CDCl_3$): δ 0.89–0.94 (3H, t, $J = 7.24$), 1.37–1.52 (2H, m), 1.65–1.72 (2H, m), 3.01 (3H, s), 3.16–3.29 (4H, dd), 4.98–5.00 (2H, ddd), 3.36–3.39 (2H, t), 3.70 (6H, s), 6.84 (2H, s), 7.38 (2H, s), 7.46 (2H, s) and 8.86–8.89 (2H, d, $J = 8.23$ Hz). Calc. for $C_{13}H_{17}N_4O_3$: C, 52.09; H, 5.97; N, 18.69. Found: C, 52.20; H, 5.79; N, 18.48%.

Me_2N-HPH-PepH_2 (3). Compound **3** was prepared using **9** as described above for **2**. IR (KBr): 3300, 2960, 1740, 1660, 1610, 1525, 1435, 1220, 1175 and 775 cm^{-1}. MS (FAB): *m*/*z* 513. ^1H NMR ($CDCl_3$): δ 2.99 (6H, s), 3.22–3.44 (4H, dd), 3.66 (6H, s), 4.92–4.94 (2H, ddd), 6.84 (2H, s), 7.41 (2H, s), 7.42 (2H, s) and 8.97–9.00 (2H, d, $J = 7.92$ Hz).

Syntheses of the copper(II) complexes

[Cu^{II}(HPH-Pep)]·2H_2O 10·2H_2O. To a solution of copper(II) acetate monohydrate (14.3 mg, 0.07 mmol) in 2 cm^3 of methanol was added dropwise a solution of 33.5 mg (0.07 mmol) of compound **1** in 5 cm^3 of methanol under agitation. The resulting blue solution was stirred at room temperature for 18 h. The methanol was then removed under vacuum, and the residue redissolved in 3 cm^3 of 2:1 (v/v) methanol–acetonitrile and filtered. Subsequent addition of 2 cm^3 of diethyl ether to the filtrate afforded light blue crystals which were recrystallized from 70% aqueous methanol solution. Yield 18 mg (45%). Calc. for $C_{21}H_{21}CuN_7O_6 \cdot 2H_2O$: C, 44.51; H, 4.45; N, 17.32. Found: C, 44.32; H, 4.40; N, 17.19%. Selected IR bands (KBr): 1735 (ν_{CO}, vs, methyl ester) and 1581 cm^{-1} (ν_{CO}, vs, imido anion).

[Cu^{II}(MeBuN-HPH-Pep)] 11. To a stirred solution of copper(II) acetate monohydrate (11.9 mg, 0.06 mmol) in 3 cm^3 of methanol was added dropwise a solution of 33.2 mg (0.06 mmol) of compound **2** in 3 cm^3 of methanol under agitation. The resulting blue solution was stirred at room temperature for 24 h. The methanol was then concentrated to one-third of its original volume. The blue solution was filtered and diethyl ether (5 cm^3) added to the filtrate. Light blue crystals formed within 24 h. They were collected by filtration, washed with diethyl ether and dried in air. Yield 29 mg (71%). Calc. for $C_{26}H_{32}CuN_8O_6 \cdot 2CH_3OH$: C, 49.44; H, 5.94; N, 16.49. Found: C, 49.64; H, 5.45; N, 16.64%. Selected IR bands (KBr): 1733 (ν_{CO}, vs, methyl ester) and 1581 cm^{-1} (ν_{CO}, imido anion).

[Cu^{II}(Me_2N-HPH-Pep)]·2CH_3OH 12·2CH_3OH. To a stirred solution of copper(II) acetate monohydrate (8.6 mg, 0.02 mmol) in 5 cm^3 of methanol was added dropwise a solution of 22.0 mg (0.04 mmol) of compound **3** in 8 cm^3 of methanol under agitation. The resulting blue solution was stirred at room temperature for 24 h. The methanol was then removed under vacuum and the residue purified by chromatography on silica gel eluted with MeOH to give complex **12**·2CH_3OH. The eluate was concentrated and the residue redissolved in 2 cm^3 of methanol and filtered. Diethyl ether was allowed to diffuse slowly into the filtrate. Light blue crystals formed within 48 h. The crystals were collected by filtration, washed with diethyl ether and dried in air. Yield 15 mg (55%). Calc. for $C_{23}H_{26}CuN_8O_6 \cdot 2CH_3OH$: C, 47.08; H, 5.38; N, 17.58. Found: C, 46.60; H, 5.29; N, 17.75%. Selected IR bands (KBr): 1733 (ν_{CO}, vs, methyl ester) and 1581 cm^{-1} (ν_{CO}, vs, imido anion).

Crystallography

Diffraction data for complex **10**·2H_2O were collected with a Rigaku AFC-5 diffractometer and graphite-monochromated Cu-Kα radiation, those for **12**·2CH_3OH with a Rigaku AFC 7R diffractometer and graphite-monochromated MoKα radiation. All the calculations were performed with the TEXSAN crystallographic software package on an Iris Indigo workstation.[8] The structures were solved by a direct method (SIR 88)[9] and expanded using Fourier techniques.[10] Scattering factors were taken from ref. 11. Non-hydrogen atoms except carbon atoms C4 and C16 and oxygen atom O17 were refined anisotropically, while C4, C16, and O17 were refined isotropically. All the hydrogen atoms were included in the models at their calculated positions but not refined. Crystal data are given in Table 2.

CCDC reference number 186/2296.

See http://www.rsc.org/suppdata/dt/b0/b006949n/ for crystallographic files in .cif format.

Physical measurements

Solution UV-vis spectra were recorded on a Hitachi UV-3000 spectrophotometer using 1 cm quartz cells, diffuse reflectance spectra of powdered samples with a Hitachi UV-4000 spectrophotometer and infrared spectra on a JEOL-6599W FT IR spectrophotometer as KBr pellets or film. EPR spectra of the frozen methanol solution at 77 K were recorded on a JEOL TE-200 spectrometer using Mn^{II}-doped MgO powder as reference ($g_3 = 2.034$ and $g_4 = 1.981$), those of the solid state on a Bruker ESP 300 spectrometer for samples copulverized with magnesium sulfate and referenced to diphenylpicrylhydrazyl (DPPH, $g = 2.0037$).

Potentiometric pH titrations. The protonation constants for ligands **1**, **2**, and **3** and complexation constants of copper(II) complexes were determined by potentiometric pH titration using a HORIBA F-7SII pH meter with 0.10 M NaOH aqueous solution at 30.0 ± 0.1 °C and the ionic strength was adjusted to 0.1 M with $NaNO_3$. The ligand concentration was 1×10^{-3} M and the ratio of metal to ligand 1 : 1. All the solutions were carefully protected from air by a stream of humidified argon. The protonation constants K_n are defined as $[H_nL]/[H_{n-1}L][H^+]$ and the 1 : 1 complexation constants ($K_{Cu^{II}H_{-2}L}$) as $[Cu^{II}(H_{-2}L)][H^+]^2/[Cu^{II}][L]$. p$K_a$ (= −log K_n) and log $K_{Cu^{II}H_{-2}L}$ were calculated according to the method described by Kodama and Kimura.[12]

Electrochemical experiments. Cyclic voltammetry (CV) was performed with a BAS-CV27 electrochemical analyzer in methanol at 30 ± 0.1 °C and the dissolved oxygen in solution was purged with argon. A three-electrode system was employed: glassy-carbon (GC) (diameter = 1 mm), Ag–AgCl (saturated KCl) and platinum wire as working, reference and auxiliary electrodes, respectively.

Results and discussion

Preparation of BuMeN-HPH-PepH$_2$ and Me$_2$N-HPH-PepH$_2$

The synthetic procedures for compounds **2** and **3** are illustrated in Scheme 1. The ligand **1** was synthesized by condensation of 2,6-pyridinedicarboxylic acid and L-histidine methyl ester by use of DPPA/DMF coupling in 74% yield. Chlorination of the acid **4** by PCl_5 in chloroform, followed by reaction with methanol, afforded dimethyl ester **5**. Hydrolysis of **5** with NaOH afforded the corresponding carboxylic acid **6** (yield 85% based on **4**). The reaction of **6** with *n*-butylmethylamine proceeded at 150 °C in a sealed tube to give the crude carboxylic acid **7**, which was converted with an excess of $SOCl_2$/MeOH into dimethyl ester **8**. The ester **8** can be reversed to **7** in quantitative yield by hydrolysis. Condensation of dicarboxylic acid **7** with L-histidine methyl ester provided **2**, which was purified by chromatography (yield 40%). Me$_2$N-HPH-PepH$_2$, **3**, was synthesized by condensation of 4-dimethylamino-2,6-pyridinecarboxylic acid and L-histidine methyl ester. IR spectra of **1**, **2**, and **3** showed strong two amide C=O stretching bands around 1660 cm^{-1}. Characterization of all the compounds was accomplished using ^{1}H NMR spectroscopy and mass spectrometry.

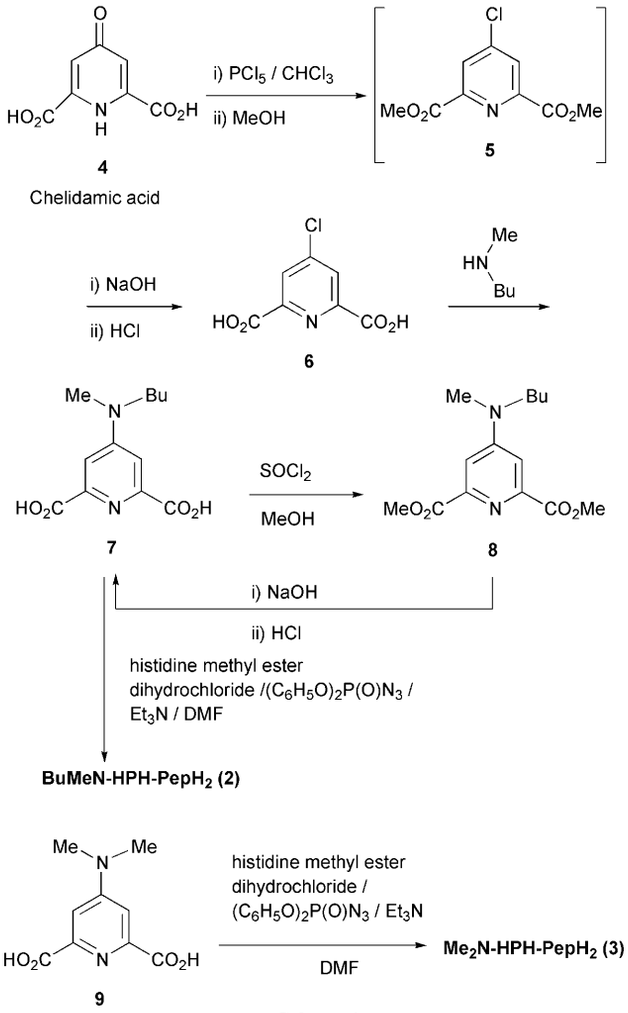

Scheme 1

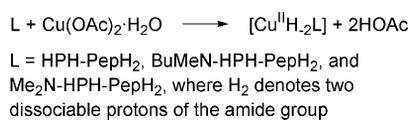

Scheme 2

Preparation of 5-coordinate copper(II) complexes (10, 11, and 12)

The preparation of complexes **10**, **11**, and **12** has been achieved by treating the corresponding "free" ligand with an equimolar amount of Cu(OAc)$_2$·H$_2$O in methanol as shown in Scheme 2. The IR spectra of these complexes showed bands at 1581 cm^{-1} being lower by *ca.* 85 cm^{-1} than those of the acid-free ligands, indicating that the two imido anions coordinate to copper(II) ion. Moreover, the elemental analyses of all the copper(II) complexes were in accord with the composition [$Cu^{II}(H_{-2}L)$], where $H_{-2}L$ denotes deprotonated amide of the ligand.

Protonation and copper(II) complexation constants for 1, 2, and 3

The protonation constants (K_n) of compounds **1**, **2**, and **3** were determined by potentiometric pH titration of 1.0 mM **1**·2HCl, **2**·3HCl or **3**·3HCl at 30 °C and $I = 0.10$ M $NaNO_3$. The titration curves of **1**, **2**, and **3** are shown in Fig. 1A-(i), 1B-(iii) and 1C-(v), respectively.

The obtained protonation constants (log K_1–K_3) are listed in Table 1 and compared with K_n values for compound **1**. For **1**·2HCl the inflection occurred at $a = 2$ (a = mol of OH^- per mol of ligand), while the inflections occurred at $a = 1$ and 2 for **2**·3HCl or **3**·3HCl. The computed log K_1–K_3 values were 6.73 and 6.05 for **1**, 6.65, 6.01, and <2 for **2**, and 6.63, 6.04, and <2 for **3**. The pK_a values of the ligands are assigned to proton loss of the imidazolyl group (log K_1 and log K_2) and the secondary amino group (log K_3). The log K_1 and log K_2 values were almost the same as those for unsubstituted **1** and *N*-β-alanyl-L-histidine (pK_a = 6.87).[13] The log K_3 of **2** and **3** are slightly lower than that of the dimethylamino group of free 4-dimethylaminopyridine (pK_a = 5)[14] due to the electron withdrawing nature of two amide groups. The protonated species are illustrated in Scheme 3.

The complexation constants for the binding of Cu^{II} with compounds **1**, **2** and **3** were determined by potentiometric pH titration of the diprotonated **1**·2H$^+$ (H_2L^{2+}) or the triprotonated **2**·3H$^+$ and **3**·3H$^+$ (H_3L^{3+}, 1 mM) with NaOH in the

Table 1 Comparison of the protonation constants[a] of pentadentate ligands **10**, **11** and **12** and copper(II) complexation constants[b]

	1	**2**	**3**
$\log K_1$	6.73	6.65	6.63
$\log K_2$	6.05	6.01	6.04
$\log K_3$		<2	<2
$\log K_{Cu^{II}H_{-2}L}$[b]	1.0	1.1	1.1

[a] $K_n = [H_nL]/[H_{n-1}L][H^+]$. [b] $K_{Cu^{II}H_{-2}L} = [Cu^{II}H_{-2}L][H^+]^2/[Cu^{II}][L]$.

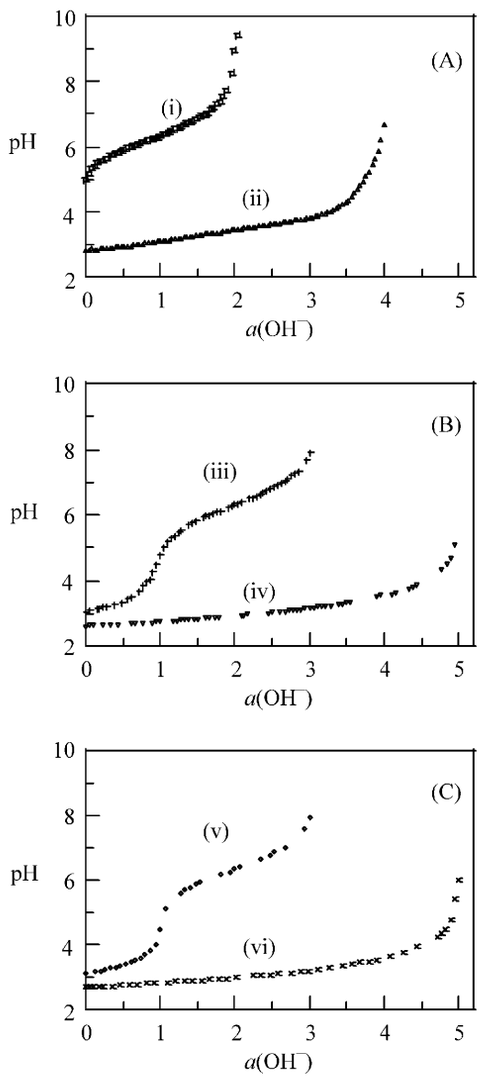

Fig. 1 pH Titration curves for the pentadentate ligands, **1**·2HCl, **2**·3HCl, and **3**·3HCl, at 30 °C with $I = 0.10$ M $NaNO_3$: (A) (i) 1.0 mM **1**·2HCl, (ii) (i) + 1.0 mM $CuSO_4$; (B) (iii) 1.0 mM **2**·3HCl, (iv) (iii) + 1.0 mM $CuSO_4$; (C) (v) 1.0 mM **3**·3HCl, (vi) (v) + 1.0 mM $CuSO_4$.

presence of an equimolar amount of Cu^{II} at 30 °C and I = 0.10 M $NaNO_3$. For the diprotonated **1**·$2H^+$, the smooth buffer curves ($0 < a < 4$) shown in Fig. 1A-(ii) indicate neutralization of the ligand is accompanied by copper(II) complexation to form 5-coordinate $[Cu^{II}(H_{-2}L)]$, **10**. On the other hand, the titration curves for triprotonated **2**·$3H^+$ or **3**·$3H^+$ with Cu^{II} (Fig. 1B-iv and 1C-vi) show a smooth buffer region at $a < 5$, indicating that loss of five protons, the two imidazolyl N, tertiary N, and two amide NH, to form five-coordinate $[Cu^{II}(H_{-2}L)]$ complexes, **11** and **12**. The 1 : 1 Cu complexation modes are as shown in Scheme 4.

From the analysis of the titration data at $a < 4$ for complex **10** or $a < 5$ for **11** and **12** the coper(II) complexation constants ($K_{Cu^{II}H_{-2}L} = [Cu^{II}(H_{-2}L)][H^+]^2/[Cu^{II}][L]$), log $K_{Cu^{II}H_{-2}L} = 1.0$ for **10**, 1.1 for **11**, and 1.1 for **12**, were determined (Table 1). The values for **11** and **12** are almost the same as that for **10**.

Table 2 Summary of crystallographic data for complexes **10**·$2H_2O$ and **12**·CH_3OH

	10·$2H_2O$	**12**·CH_3OH
Formula	$C_{21}H_{25}CuN_7O_8$	$C_{12.50}H_{16}Cu_{0.5}N_4O_6$
M	567.0	318.06
Crystal system	Tetragonal	Orthorhombic
Space group	$P4_32_12$ (no. 94)	$C222_1$ (no. 20)
a/Å	16.854(5)	14.178(3)
b/Å	16.854(5)	16.111(2)
c/Å	19.824(9)	13.676(3)
V/Å^3	5631(3)	3123.9(8)
T/K	293	293
Z	8	8
μ/cm^{-1}	162.6	7.56
Reflections collected	2548	2067
Independent reflections	2548	2008
R_1 [$I > 2\sigma(I)$]	0.0791	0.071
$wR2$ [$I > 2\sigma(I)$]	0.2103	0.072

Table 3 Selected bond distances (Å) and angles (°) for complexes **10**·$2H_2O$ and **12**·$2CH_3OH$

	10	**12**
Cu–N(1)	1.929(6)	1.91(2)
Cu–N(8)	2.002(7)	1.99(1)
Cu–N(8*)	2.072(7)	1.98(1)
Cu–N(12)	2.072(7)	2.05(1)
Cu–N(12*)	2.119(7)	2.05(1)
N(1)–Cu–N(8)	79.9(3)	80.0(3)
N(1)–Cu–N(12)	138.9(3)	127.3(4)
N(1)–Cu–N(8*)	78.7(3)	80.0(3)
N(1)–Cu–N(12*)	119.2(3)	127.3(3)
N(8)–Cu–N(12)	90.0(3)	89.6(4)
N(8)–Cu–N(8*)	158.6(3)	160.0(6)
N(8)–Cu–N(12*)	104.2(3)	102.6(4)
N(12)–Cu–N(8*)	106.2(3)	105.4(7)
N(12)–Cu–N(12*)	101.9(3)	105.4(7)
N(8*)–Cu–N(12*)	86.4(3)	89.6(4)

Crystal structure of complex 10·$2H_2O$

A preliminary report on the structure of complex **10**·$2H_2O$ was communicated earlier.[7] Here the data from further refinement are described. The green crystals suitable for X-ray diffraction study were obtained by slow evaporation of a 60–70% aqueous methanol solution. Crystallographic data are presented in Table 2. The ORTEP[15] drawing of **10** is shown in Fig. 2, and selected bond distances and angles are listed in Table 3. The coordination geometry around the central Cu atom is distorted square pyramidal with $\tau = 0.33$ (structural parameter $\tau = (\beta - \alpha)/60$), where α and β are the two basal angles ($\beta \geqslant \alpha$), represents the change in trigonal distortion from square pyramidal geometry: $\tau = 0$ for an ideal square pyramid, 1 for an ideal trigonal bipyramid).[16] One pyridyl nitrogen N(1), one imidazolyl nitrogen N(12), and two deprotonated nitrogens (N(8) and N(8*)) make the basal plane while one imidazolyl nitrogen N(12*) occupies the apical position. The Cu atom lies 0.35 Å above the basal plane towards the apical nitrogen N(12*). The two deprotonated N(8) and N(8*) and the pyridine ring are essentially coplanar and two N–Cu–N angles (average 79.0°) in two five-membered chelate rings are smaller than the ideal angle 90° of a square pyramid.

The N(8)–Cu–N(12) angle is 90.0(3)° while the N(8)–Cu–N(12*) is slightly larger (104.2(3)°). The N(1)–Cu–N(12) angle (138.9(3)°) is significantly less than the ideal angle 180°, being indicative of some distortion toward a trigonal bipyramid.

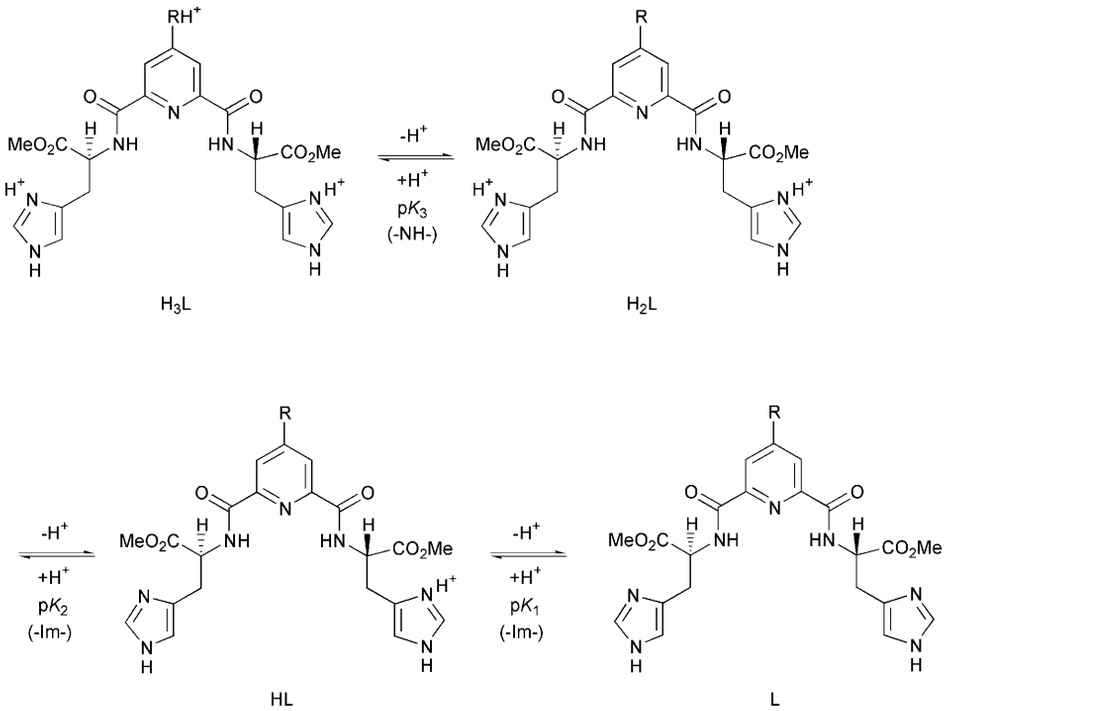

Scheme 3

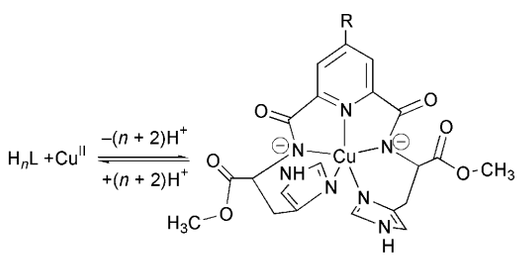

10: L = HPH-PepH$_2$ **(1)**; n =2

11: L = BuMeN-HPH-PepH$_2$ **(2)**; n= 3

12: L = Me$_2$N-HPH-PepH$_2$ **(3)**; n =3

Scheme 4

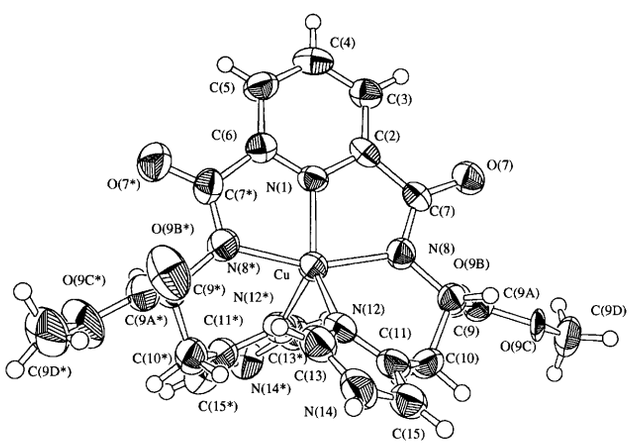

Fig. 2 ORTEP drawing of complex **10**, with atom-labeling scheme. The thermal ellipsoids are drawn at the 50% level.

The Cu–N(1) (pyridine) and Cu–N(8) and –N(8*) (amide) bond distances are 1.929(6), 2.002(7), and 2.072(7) Å for complex **10** and are similar to those of $[Cu^{II}(H_{-1}L^2)]^+$ (1.930(3) Å, L^2 = 2-[((2-(4-imidazoyl)ethyl)amino)carbonyl]-6-[((2-amino-2-carbamoylethyl)amino)methyl]pyridine),[17] $[Cu^{II}(H_{-1}L^3)]^+$ (1.946(4) Å, L^3 = 2-[((2-(4-imidazoyl)ethyl)amino)carbonyl]-6-[((2-amino-2-methylpropyl)amino)methyl]pyridine),[18] $[Cu^{II}(H_{-1}L^4)]^+$ (1.937(5) Å, L^4 = 2-[((2-(1-imidazoyl)ethyl)amino)-carbonyl]-6-[((2-amino-1,1,2-trimethylpropyl)amino)methyl]-pyridine),[18] [Cu{P(C$_5$H$_4$N-2)$_3$}] (1.942(2) Å)[18] and [Cu{P(pz)$_2$(C$_5$H$_4$N-2)}] (Hpz = pyrazole) (1.928(2) Å).[19]

The average Cu–N (amide) distance of complex **10** (2.04 Å) is in the normal range for copper(II) complexes of glycine-L-histidine[20] and glycyl-L-histidylglycine[21] (1.93–1.98 and 1.93–1.99 Å, respectively). The apical Cu–N(12*) distance (2.119(7) Å) is slightly longer than that of equatorial Cu–N(12) (2.072(7) Å) due to the Jahn–Teller effect, but they are close to those found in related copper(II) complexes.[8,16,20,21]

The dihedral angle of the two imidazolyl rings is 63.60°, a little larger than that of 57.09° for complex **12**.

Crystal structure of complex 12·2CH$_3$OH

The blue crystals suitable for X-ray diffraction study were obtained by slow vapor diffusion of diethyl ether into a methanolic solution. Crystallographic data are presented in Table 2. The ORTEP drawing of complex **12**·2CH$_3$OH is shown in Fig. 3, and selected bond distances and angles are listed in Table 3. The geometry around the copper centre in **12** is intermediate between a square pyramid and a trigonal bipyramid with τ = 0.55 (α = 127.3(3)° and β = 160.0(6)°).

All the Cu–N bond distances (average 1.98 Å) for complex **12** are comparable to those of **10** (average 2.0 Å). The distortion from the ideal square pyramidal geometry, however, is much larger than in **10**, with the greatest deviation being N(1)–Cu–N(12) 127.3(4)° (138.9(3)° for **10**), which is due to the N(8*)–Cu–N(12) angle of 105.4(7)° (106.2(3)° for **10**). The trigonal angles at N(1), N(12), and N(12*) are inequivalent: two larger and one less than 120°.

Thus, the introduction of the dimethylamino group to pyridine leads to distortion from a square pyramidal toward a trigonal bipyramidal geometry.

EPR Studies

The EPR spectra of complexes **10**, **11**, and **12** at 77 K are shown in Fig. 4. The spectrum of **10** was typical of an axially symmetrical complex with $g_\parallel > g_\perp$ ($g_\parallel$ = 2.218, $g_\perp$ = 2.049, $A_\parallel$ = 15.3 mT) and a $d_{x^2-y^2}$ ground-state doublet. On the other hand the spectra of **11** and **12** were different from that of

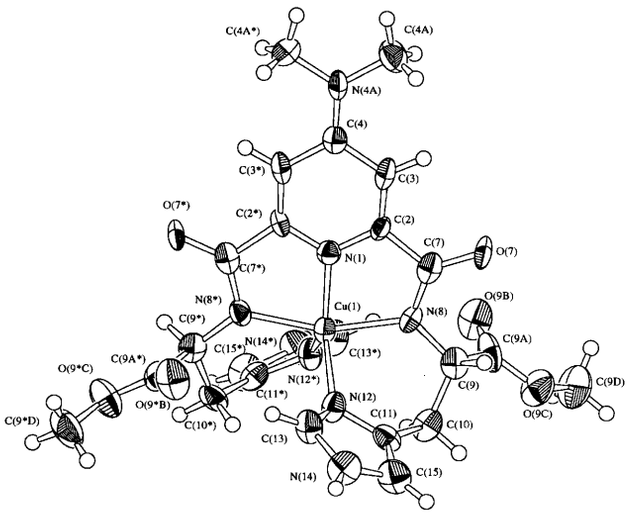

Fig. 3 ORTEP drawing of complex **12**. Details as in Fig. 2.

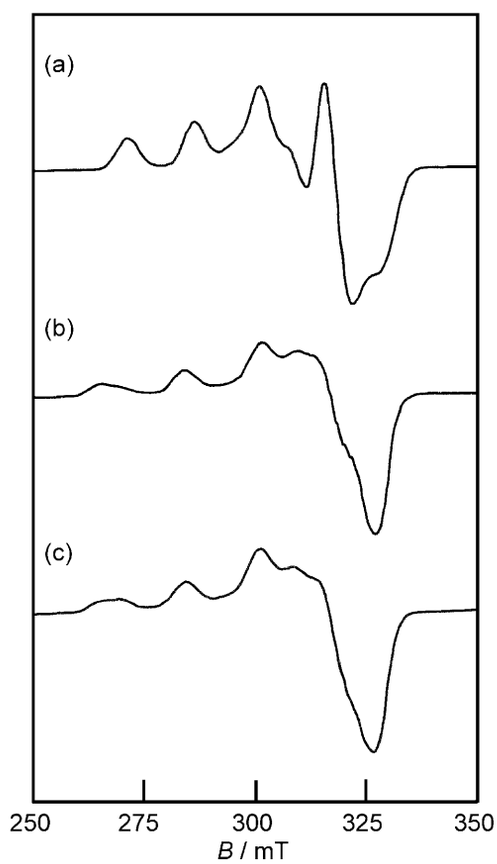

Fig. 4 X-Band EPR spectra of complexes **10** (a), **11** (b), and **12** (c) in methanol glass at 77 K.

10 and their parameters were $g_{\|} = 2.229$, $g_{\perp} = 2.057$, $A_{\|} = 17.13$ mT for **11** and $g_{\|} = 2.227$, $g_{\perp} = 2.058$, $A_{\|} = 17.13$ mT for **12**. A feature of the spectra is the marked increase in $A_{\|}$ in the case of **11** and **12**. This suggests that there is less distortion than in **10**.

In contrast, the EPR of complexes **10** and **12** measured as powders (100 K) show isotropic signals at $g_{iso} = 2.046$ with linewidth, ΔB_{pp}, of 12.5 mT for **10** and at 2.114 with $\Delta B_{pp} =$ 8.7 mT for **12**, respectively; these linewidths are typical of powdered monomeric copper(II) complexes[22–24] and both complexes would appear to adopt almost the same geometry as that found in the crystal structures.

Electronic absorption spectra

The absorption spectra of complexes **10**, **11**, and **12** in methanol

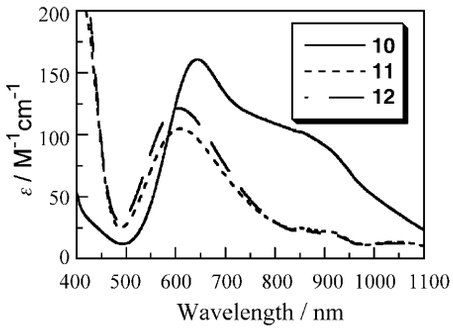

Fig. 5 Electronic absorption spectra of complexes **10** (——), **11** (- - - -), and **12** (— —) in methanol–water (1 : 1 v/v) at 25 °C.

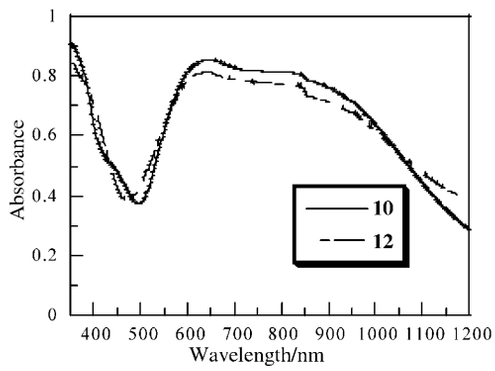

Fig. 6 Diffuse reflectance spectra of complexes **10** (——) and **12** (— —) at 25 °C.

(Fig. 5) exhibited absorption maxima λ_{max} at 641 nm (ε 161) with a shoulder at *ca.* 900 nm (ε 92 M^{-1} cm^{-1}) for **10**, at 609 (ε 105) and 900 nm (ε 22 M^{-1} cm^{-1}) for **11**, and at 605 (ε 122) and 900 nm (ε 21 M^{-1} cm^{-1}) for **12** respectively (Table 4). These spectra are characteristic of tetragonally distorted copper(II) complexes where the bands arise from absorption maxima at 641, 609, and 605 nm and the shoulder bands around 900 nm are assigned to the d_{xz}, $d_{yz} \longrightarrow d_{x^2-y^2}$ and the $d_{xy} \longrightarrow d_{x^2-y^2}$ transitions.[25] The lower energy absorption maxima and the high absorption coefficient around 900 nm observed for **10** indicate a weak in-plane field strength compared with those of **11** and **12**. Moreover, the red shift of **10** by 32–36 nm compared to **11** and **12** suggested that its geometry is distorted toward trigonal bipyramidal in solution. Thus, the spectral data of **10** are consistent with the degree of deviation from ideal square pyramidal geometry found with EPR spectroscopy.

For complexes **10** and **12**, the diffuse reflectance spectra were similar to each other as shown in Fig. 6 with a maximum around 630–650 nm and a shoulder around 900 nm, and reflect the intermediacy of the solid structures between square pyramid and trigonal bipyramid extremities. The difference of absorption maxima between **10** (638 nm) and **12** (646 nm) is ascribed to the distortion of **12** towards a trigonal bipyramid in solution. A similar behavior has been observed by Spiccia and co-workers in five-coordinate copper(II) complexes of the pentadentate ligands trenimpy (3-[4-(2-pyridyl)-3-aza-3-butenyl]-3-azapentane-1,5-diamine) and trenpy (3-[4-(2-pyridyl)-3-azabutyl]-3-azapentane-1,5-diamine).[26]

Electrochemistry

The effects of introducing electron donating substituents such as Me_2N or MeBuN to the pyridine ring of compound **1** were reflected in the redox properties of the copper(II) complexes. The electrochemical properties of **10**, **11**, and **12** were studied by cyclic voltammetry in methanol with tetrabutylammonium perchlorate as the supporting electrolyte at 30 °C. An irreversible oxidation wave was observed at $E_{pa} = +0.99$ V for **10**, +1.16 V for **11** and **12**. The oxidation potential for **11** and **12** is

Table 4 Physical properties of copper(II) complexes **10**, **11**, and **12**

Complex	Medium	vis	EPR					
		λ_{max}/nm (ε/M^{-1} cm^{-1})	g_{iso}	$g_{\perp}$	$g_{\parallel}$	$A_{\parallel}$/mT	A_N/mT	E_{ox}/V *vs.* Ag–AgCl
10	Solid	638	2.046					
	Methanol	641 (161), 900sh (92)		2.049	2.218	15.30	not detected	+0.99 (irr.)[a]
11	Methanol	609 (105), 900sh (22)		2.057	2.229	17.13	1.66	+1.16 (irr.)[a]
12	Solid	646	2.114					
	Methanol	605 (122), 900sh (21)		2.058	2.227	17.13	1.50	+1.16 (irr.)[a]

[a] irr. = Irreversible.

close to those of copper(II) complexes of dipeptides.[27] However, it is shifted anodically by 170 mV relative to the non-substituted five-coordinate **10**, indicating that the copper(II) species is stabilized.

Conclusion

We have prepared three peptide ligands having a pyridine and two histidine moieties that stabilize five-coordinate copper(II) complexes. The crystal structures of **10** and **12** revealed that introduction of the secondary amino substituent is sufficient to change the geometry around Cu^{II} from square pyramidal toward trigonal bipyramidal in the crystalline state. On the other hand, as indicated by UV-visible absorption spectra and/or EPR, the coordination geometry in solution changes by successive introduction of the secondary amino substituent from trigonal bipyramidal to square pyramidal in contrast to the crystalline state. Finally, the introduction of an electron-donating substituent such as Me_2N or MeBuN to the pyridine ring influences the geometry around the copper(II) and causes the compounds to exhibit spectroscopic and electrochemical properties different from those of the non-substituted complex **10**.

References

1 J. Cohen, *Science*, 1997, **277**, 32.
2 J. K. Wong, M. Hezareh, H. F. Gunthard, D. V. Havlir, C. C. Ignacio, C. A. Spina and D. D. Richman, *Science*, 1997, **278**, 1291.
3 D. Finzi, M. Hermankova, T. Pierson, L. M. Carruth, C. Buck, R. E. Chaisson, T. C. Quinn, K. Chadwich, J. Margolick, R. Brookmeyer, J. Gallant, M. Markowitz, D. D. Ho, D. D. Richman and R. F. Silliciano, *Science*, 1997, **278**, 1295.
4 M. Fujita, M. Otsuka and Y. Sugiura, *J. Med. Chem.*, 1998, **39**, 503.
5 M. Otsuka, M. Fujita, T. Aoki, S. Ishii, Y. Sugiura, T. Yamamoto and J. Inoue, *J. Med. Chem.*, 1995, **38**, 3264.
6 M. Otsuka, M. Fujita and Y. Sugiura, *J. Med. Chem.*, 1994, **37**, 4267.
7 M. Otsuka, H. Satake, S. Murakami, M. Doi, T. Ishida, Y. Shibasaki and Sugiura, *Bioorg. Med. Chem.*, 1996, **4**, 691.
8 TEXSAN, Crystal Structure Analysis Package, Molecular Structure Corporation, Houston, TX, 1985 and 1992.
9 SIR 88, M. C. Burla, M. Camalli, G. Cascarano, C. Giacovazzo, G. Polidori, R. Spagna and D. Viterbo, *J. Appl. Crystallogr.*, 1989, **22**, 389.
10 DIRDIF 94, P. T. Beurskens, G. Admiraal, G. Beurskens, W. P. Bosman, R. de Gelder, R. Israel and J. M. M. Smits, Technical Report of the Crystallography Laboratory, University of Nijmegen, 1994.
11 D. T. Cromer and J. T. Waber, *International Tables for X-Ray Crystallography*, Kynoch Press, Birmingham, 1974, vol. IV.
12 M. Kodama and E. Kimura, *J. Chem. Soc.*, *Dalton Trans.*, 1979, 325.
13 Z. M. Kurtyku, *Handbook of Chemistry and Physics*, ed. R. C. Weast, CRC Press, Boca Raton, FL, 1985–1986, 66th edn., p. D-159.
14 The protonation constant for 4-dimethylpyridine dihydrochloride salts was determined by potentiometric pH titration with $I = 0.10$ M $NaNO_3$ at 30 °C.
15 C. K. Johnson, ORTEP-II, Report ORNL-5138, Oak Ridge, National Laboratory, Oak Ridge, TN, 1976.
16 A. W. Addison, T. N. Rao, J. Reedijk, J. van Rijn and G. Verschoor, *J. Chem. Soc.*, *Dalton Trans.*, 1984, 1349.
17 E. Kimura, H. Kurosaki, Y. Kurogi, M. Shionoya and M. Shiro, *Inorg. Chem.*, 1992, **31**, 4314.
18 F. A. Chavez, M. M. Olmstead and P. K. Mascharak, *Inorg. Chem.*, 1996, **35**, 1410.
19 F. A. Chavez, M. M. Olmstead and P. K. Mascharak, *Inorg. Chim. Acta*, 1998, **269**, 269.
20 J. F. Blount, K. A. Fraser, H. C. Freeman, J. T. Szymanski and C. H. Wang, *Acta Crystallogr.*, 1967, **22**, 396.
21 R. Osterberg, B. Sjoberg and R. Soderquist, *Acta Chem. Scand.*, 1972, **26**, 4184; P. de Meester and D. J. Hodgson, *Acta Crystallogr.*, *Sect. B*, 1977, **33**, 3505.
22 C. J. Harding, Q. Lu, J. F. Molone, D. J. Marrs, N. Martin, V. Mckee and J. Nelson, *J. Chem. Soc.*, *Dalton Trans.*, 1995, 1739.
23 I. M. Procter, B. J. Hathaway and P. Nicholls, *J. Chem. Soc. A*, 1968, 1678.
24 J. F. Boas, J. R. Pilbrow, G. J. Troup, C. Moore and T. D. Smith, *J. Chem. Soc. A*, 1969, 965.
25 B. J. Hathaway and A. A. G. Tomlinson, *Coord. Chem. Rev.*, 1970, **5**, 1.
26 G. A. McLachlan, G. D. Fallon, R. L. Martin and L. Spiccia, *Inorg. Chem.*, 1995, **34**, 254.
27 F. Fabbrizzi, A. Perotti and A. Poggi, *Inorg. Chem.*, 1983, **22**, 1411; T. Sakurai, J.-I. Hongo, A. Nakahara and Y. Nakao, *Inorg. Chim. Acta*, 1980, **46**, 205; S. T. Kirksey Jr., T. A. Neubecker and D. W. Margerum, *J. Am. Chem. Soc.*, 1979, **101**, 1631; E. Kimura, T. Koike, R. Machida, R. Nagai and M. Kodama, *Inorg. Chem.*, 1984, **23**, 4181.